

Incorporating temporal dynamics of mutations to enhance the prediction capability of antiretroviral therapy's outcome for HIV-1

Giulia Di Teodoro^{a,b}, Martin Pirkl^{c,d}, Francesca Incardona^{b,e}, Ilaria Vicenti^f, Anders Sönnerborg^{g,h}, Rolf Kaiser^{c,d}, Laura Palagi^a, Maurizio Zazzi^f and Thomas Lengauer^{c,i}

^aSapienza University of Rome, Department of Computer Control and Management Engineering Antonio Ruberti, 00185, Rome, Italy

^bEuResist Network, 00152, Rome, Italy

^cUniversity of Cologne, Institute of Virology, Faculty of Medicine and University Hospital Cologne, 50935, Cologne, Germany

^dPartner Site Cologne-Bonn, German Center for Infection Research (DZIF), 50935, Cologne, Germany

^fUniversity of Siena, Department of Medical Biotechnologies, 53100, Siena, Italy

^eI-PRO, 00152, Rome, Italy

^gKarolinska Institutet, Division of Infectious Diseases, Department of Medicine Huddinge, 14152, Stockholm, Sweden

^hKarolinska University Hospital, Department of Infectious Diseases, 14186, Stockholm, Sweden

ⁱMax Planck Institute for Informatics, Saarland Informatics Campus, Computational Biology, 66123, Saarbrücken, Germany

ARTICLE INFO

Keywords:

human immunodeficiency virus
antiretroviral drug
therapy prediction
rate of mutation disappearance
weighting factors for mutations
viral load
Stanford mutation-drug resistance score
machine learning

ABSTRACT

Motivation: In predicting HIV therapy outcomes, a critical clinical question is whether using historical information can enhance predictive capabilities compared with current or latest available data analysis. This study analyses whether historical knowledge, which includes viral mutations detected in all genotypic tests before therapy, their temporal occurrence, and concomitant viral load measurements, can bring improvements. We introduce a method to weigh mutations, considering the previously enumerated factors and the reference mutation-drug Stanford resistance tables. We compare a model encompassing history (H) with one not using it (NH).

Results: The H-model demonstrates superior discriminative ability, with a higher ROC-AUC score (76.34%) than the NH-model (74.98%). Significant Wilcoxon test results confirm that incorporating historical information improves consistently predictive accuracy for treatment outcomes. The better performance of the H-model might be attributed to its consideration of latent HIV reservoirs, probably obtained when leveraging historical information. The findings emphasize the importance of temporal dynamics in mutations, offering insights into HIV infection complexities. However, our result also shows that prediction accuracy remains relatively high even when no historical information is available.


Supplementary information: Supplementary material is available.

Introduction

Human immunodeficiency virus (HIV), if untreated, is a deadly pathogen. While there are treatment options, there is still no cure or vaccine. Since its discovery in 1981, 84.2 [64.0-113.0] million people have been infected with HIV, claiming about 40.1 [33.6-48.6] million lives. By the end of 2022, about 39.0 million people were living with HIV [18]. Early diagnosis and proper treatment offer life expectancy comparable to HIV-negative individuals. HIV-1 infection requires antiretroviral treatment; without it, patients eventually develop acquired immunodeficiency syndrome (AIDS). Standard care involves the administration of cocktails of antiretroviral drugs, rather than one individual medicine, to minimize the risk of emergent drug resistance. Antiretroviral therapies against HIV-1 can lead to the selection of drug-resistant HIV-1 variants that can spread between hosts, causing treatment failure [11][36]. Resistance testing can help to suppress viral replication and to prevent the transmission of resistant variants. The study of the susceptibility of the HIV-1 variants to available antiretroviral drugs can be done by genotypic testing or phenotypic testing [32]. Phenotypic testing directly measures the drug concentration required

to inhibit virus replication in vitro, while genotypic testing reads the viral genome and infers drug susceptibility based on prior knowledge of resistance mutations. Genotypic resistance tests, being the more practical variant, are routinely used in clinical practice. If drug-resistant viral variants emerge, therapy must be replaced with a different drug combination to suppress replication. Clinicians grapple with identifying new drug combinations to suppress HIV replication, taking into account viral drug resistance, previous successful and failing therapies, and retention of future treatment options. However, the latent viral population in the patient living with HIV (PLWH) accumulates a large number of resistance-associated mutations, which may not be observable in blood serum but rapidly reappear when it is advantageous, i.e., under the appropriate drug pressure [25][36]. The many possible drug combinations complicate therapy selection, especially in advanced stages. For this reason, over the years genotypic interpretation systems for drug resistance have been developed to predict the success or failure of antiretroviral drug regimens.

Genotypic drug resistance interpretation systems (GIS) are rule-based or algorithm-driven interpretation systems. The former approach uses expert-driven tables of drug-resistance

 giulia.diteodoro@uniroma1.it (G. Di Teodoro)

mutations [37] to assign drug-resistance scores to genotypes that describe drug resistance. Several rules sets have been developed over the years by experts, such as the ones from ANRS, HIVdb [31], HIV-GRADE, and the Rega Institute, all available on the HIV-GRADE website [17]. These rule-based systems are continually updated collaboratively with consistent changes in HIV drug resistance knowledge, treatment guidelines, and expert opinion [20]. All these systems interpret data obtained from Sanger sequencing, a long-standing technology widely used thanks to its low rate of error and its cost-effectiveness. However, this technique has limits in detecting minor resistant populations [6][33] that could have clinical relevance [5][35]. Higher resolution sequencing techniques, collectively referred to as next-generation sequencing (NGS) [7], are now being increasingly used which can detect minority variants representing as low as 1% of the viral population, as opposed to roughly 20% with Sanger sequencing. The mutational patterns detected by NGS are currently subjected to the same genotype interpretation systems as those detected by Sanger sequencing. However, the clinical role of drug resistance mutations at 1% to 20% prevalence is still a matter of debate and is likely different for different drugs and mutations. On the other hand, data-driven genotypic interpretation systems rely on statistical or ML methods to infer drug resistance directly from data. Due to the large amount of clinical and genotypic data available, data-driven GIS systems have become a prominent approach to help clinicians choose effective HIV therapies, especially for heavily treatment-experienced patients with complex drug resistance patterns that have evolved over the years. Early data-driven GISs, like the Virco proprietary VirtualPhenotypeTM [34] and the geno2pheno system [2], predict the *in-vitro* phenotype. The Virco system (VircoTYPE) was initially based on a linear regression model that estimates the phenotypic measurement as the weighted sum of the effects of individual mutations and then updated in a way that the predicted phenotype is translated into a clinically relevant estimate of efficacy [39]. Geno2pheno initially assessed virus resistance to individual compounds (Geno2pheno[*resistance*]) and later predicted virological responses to 3-4 drug AntiRetroviral Therapy (ART) regimens. Geno2pheno-THEO estimated treatment success probability using genotypic data and user inputs [1]. Geno2pheno[*resistance*] [23] [13] uses sequences and drug data for classification through SVM, evaluating the distances from the decision boundaries to estimate drug-specific resistance. Geno2pheno[*drug exposure*] [22] uses the same input first to produce drug exposure scores (DESS) correlated with prior drug exposure and secondly to supply the probabilities of exposure derived from the produced DESS into the therapy model. Another software developed to infer the virological response to antiretroviral drug regimen is SHIVA which employs random forests [26]. In one study, artificial neural networks were used for the same purpose [12].

Some research suggests that mutations that have been observed in the past and then disappeared from blood serum

can impact a patient's current status and the effectiveness of subsequent therapy. The time since a mutation first appeared or disappeared from blood serum may influence the degree to which that mutation informs a patient's status and resistance to antiretroviral drugs [4, 8]. On addition, the impact of a mutation is thought to be more important the higher the viral load (VL) when the mutation was observed. In light of these considerations, in our model, we consider not only the mutations detected by the patient's most recent genotypic resistance test (GRT), as in models currently in routine use. We consider the entire history of mutations recorded for the patient in the database before the therapy of interest, for which we want to correctly predict the success or failure for that particular patient. Mutations contribute additively to the patient's resistance status. The contribution of each mutation is multiplied by a weight that incorporates (i) a degression factor for time: the further back in time the mutation was observed, the less likely it is to be still influential in determining the patient's drug resistance, (ii) the area under the VL curve measured in a time window around the date of the mutation's occurrence: the larger that area the more informative the mutation is considered to be, (iii) a penalty score based on the HIVdb system, in which each Drug Resistance Mutation (DRM) is assigned a drug penalty score based on medical expertise, widely recognized in the literature. Since the latent virus in organ tissue is not accessible to routine diagnostics, with this methodology, we aim to infer hidden mutations from history data on mutations seen in blood serum. Moreover, our system is based on a single support vector machine (SVM) model that predicts the therapy outcome from the patient's mutation history.

Methods

Problem setting

Let $\mathbf{M} = \{1, \dots, M\}$ ($M = 5941$) be the set of mutations considered, $m \in \mathbf{M}$, denote a specific mutation, and $date_m$ the most recent point in time when that mutation was recorded in a GRT. Let $\mathbf{D} = \{1, \dots, D\}$ be the set of drugs considered and $d \in \mathbf{D}$ denote an individual drug. Let $r \in \{0, 1\}^M$ be a vector indicating all DRMs observed in at least one viral genotype before the onset of the therapy of interest. Eventually, the mutations this vector indicates ($r_i = 1$) will be weighted with the weighting factors explained in the subsequent section. Let $z \in \{0, 1\}^D$ be a vector indicating the combination of drugs used in a particular therapy of interest, and let $start_z$ denote the time point of the onset of therapy z . Label $y \in \{0, 1\}$ indicates success (0) or failure (1) of the therapy. The definition of success or failure of therapy is given in defining the Standard Datum. The model is therapy-oriented, such each datapoint in the training set is made up of the i^{th} *patient-therapy* pair $x_i = (r_i, z_i)$ and the corresponding value of the output y_i ; hence it is a triple (r_i, z_i, y_i) . Let $\mathbf{T} = \{(r_1, h_1, y_1), \dots, (r_N, h_N, y_N)\}$ be the training set, where N is the cardinality of the set of patient-therapy pairs. Our goal is to train a model $f(x)$ that

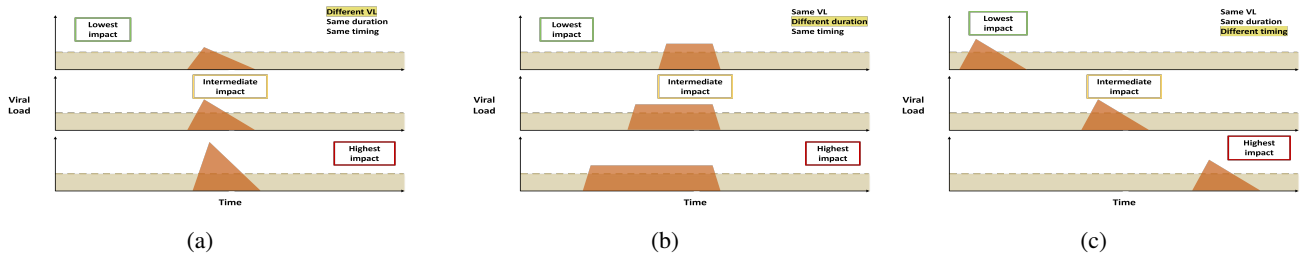


Figure 1: Figure (a) represents how different viral loads, measured when a mutation was detected, can impact present drug resistance. Figure (b) represents how different durations of a mutation can impact present drug resistance. Figure (c) represents how different mutation timing can impact present drug resistance.

accurately predicts the outcome of a target therapy z , using information from the patient's past medical history.

The weighting factors of the mutations

Previous experience suggests that the timing and duration of mutations could affect therapy efficacy. In addition, the magnitude of VL when a mutation is detected could influence viral replication. How these factors could impact the present drug resistance is shown schematically in Figure 1. This is precisely why these factors are incorporated in the calculation of the weight factor for a mutation. In addition, the Stanford Score table is also taken into account. This is a table of scores indicating the impact of individual mutations on drug resistance of the virus. The scores for the mutations observed in a viral genotype are accumulated to yield an overall score quantifying the drug resistance of the virus to an ART regimen. The Stanford Score table is widely used as an independent predictor of virologic response to drug regimens [31].

Time. The closer the last time point that a mutation has been observed lies to the initiation of a drug regimen, the greater its impact on the efficacy of this regimen is assumed to be. The reason is that the covert reservoir of provirus in tissues is assumed to deplete over time. We modeled the rate of disappearance of a mutation via a sigmoid curve: for a certain period of time, the mutation has a high propensity of impacting drug resistance, then this propensity begins to decline, tending to zero. To learn the onset of the decline of the curve α_m and slope β_m of each sigmoid curve $y(t) = \frac{1}{1+e^{\alpha+\beta t}}$ pertaining to an individual mutation, the data on when mutations were and were not observed, respectively, were collected as explained below.

The mutations were grouped by drug class (Protease Inhibitor (PI), Nucleoside Reverse Transcriptase Inhibitor (NRTI), Non-Nucleoside Reverse Transcriptase Inhibitor (NNRTI), Integrase inhibitor (INI)). To assess the rate of disappearance of a mutation, one has to consider periods when the patient is not on ART or is not taking any drug of a given drug class that might select for that mutation. Consider, for example, mutations in the PI drug class. Starting with the entire database, we take all patients who

had a therapy with at least one drug of the PI class (PI therapy) and immediately after a period when they were on another therapy that contained no drug of the PI class or a period where the patient was not under any therapy so that there was no drug pressure due to any drug from the PI class in the patient. If we consider all the PI mutations present in the genotypic sequences during the therapy, including one or more PIs, we can see how many of those mutations disappeared at some point in one of the gene sequences that were sampled in the subsequent period. If a mutation was present during the PI therapy, the following cases might occur:

- In the first sequence sampled after the PI therapy was stopped, the mutation has already disappeared. The mutation's persistence period is assumed to be the time between the date the PI therapy was stopped and the date this sequence was sampled.
- The mutation is still present in the first sequence after discontinuing the PI therapy but disappears in the n^{th} sequence observed. Here, the persistence period is the time between the date of discontinuation of PI therapy and the date of sampling of the n^{th} sequence.
- The mutation is present in all subsequent sequences until the end of the period when the patient is no longer free of a PI drug, so we consider that the mutation has not disappeared.

Therefore, for the m^{th} mutation, we construct two vectors:

- The vector x_m of days elapsed from the date of discontinuation of the PI therapy to the sampling date of gene sequences at a later time point when the patient experiences no drug pressure due to drugs in the PI class (e.g., $x_m = [20, 50, 250, 347, 500, 1000]$ would represent a sequence of six consecutive GRTs that occur at the indicated number of days after stopping a PI therapy, i.e., the first test happens at day 20, the second at days 50, etc).
- The vector of binary values indicating whether, at each time point indicated by the vector x_m , the mutation is present (1) or has not been observed (0). (e.g.,

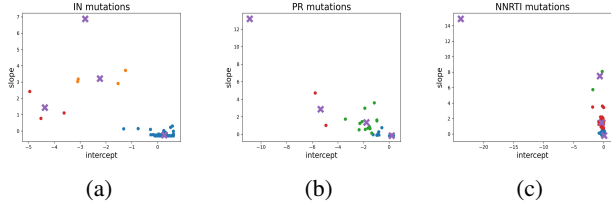


Figure 2: Figure (a) is the slope-intercept pairs clustered for IN-mutations, Figure (b) is the slope-intercept pairs clustered for PR-mutations and Figure (c) is the slope-intercept pairs clustered for NNRTI-mutations.

$y_m = [1, 1, 1, 1, 0, 0]$, corresponding to the vector of the previous example, indicates that the m^{th} -mutation is present in the first 4 GRTs performed after therapy stop, but in the fifth test, after 500 days, is no longer there. In the data, there are also situations in which, e.g., $y_m = [1, 1, 1, 0, 1, 0]$ where the mutation reappears.

Let $x = (x_1, \dots, x_n)$ be a random sample of n observations from the distribution with *probability distribution function* (*p.d.f* or *pdf*) $f(x; \theta) = \frac{1}{1+e^{(\alpha+\beta x)}}$ depending on a parameter $\theta = (\alpha; \beta)$. We defined the target probabilities $t_m = \frac{y_m+1}{2}$ and minimized the negative log-likelihood function [24]

$$\min_{\theta} -\frac{1}{n} \sum (t \log(f(x; \theta)) + (1-t) \log(1-f(x; \theta)))$$

Equipping our statistical model for therapy efficacy with individual degeneration curves for each mutation is not promising, given the small amount of data we have. Thus, we decided to cluster the slope-intercept pairs of the curves for mutations pertaining to a drug class with a *k-means* algorithm after standardizing them using the *z-score*.

This procedure was repeated for mutations pertaining to all drug classes, except for the NRTI class, because drugs from this class have been administered practically always without interruption. The clusters are depicted in Figures 2a, 2b and 2c, where the points represent the slope-intercept pairs, the colors refer to the different clusters and the crosses represent the clusters' centroids. For mutations for which no data were available to learn the slope and intercept of the sigmoid functions, the slope and the intercept of their sigmoid curves are treated as hyper-parameters of the model to be optimized by cross-validation.

Viral load. The results in previous studies [14] suggest that the viral load observed in the presence of a mutation could influence the impact that the mutation has on drug resistance. To take this into account, since a value of the VL is not always present for the same day that the genetic sequence was sampled for GRT, it was decided to consider a two-month time window around the date the genetic sequence was sampled and to use the area under the viral load curve obtained by performing linear interpolation of the viral load values measured within that time window. We

will refer to this area as $Area_{VL}$. Note that the viral load values were logarithmized and decreased by $\log(50)$ such that VLs values below $50cp/ml$ contribute a negative area. The rationale is that 50 is the threshold of undetectability currently used in clinical routine.

The Stanford Score. The Stanford score is associated with a mutation-drug pair, $s_{m,d}$. This score is higher the more a given mutation decreases the susceptibility of the virus to the drug. Not all mutations are considered in the Stanford tables; therefore, for those for which this information is not available, the score is set to 0. If a mutation is associated with multiple drugs (across drug classes) included in the drug regimen z_i and therefore multiple Stanford scores apply, the minimum Stanford score is used, because the most effective drug can be assumed to dominate the effect on the virus. To fend against biases introduced by learning on largely differing values all scores were standardized by dividing them by the norm of the vector of all possible Stanford score $s = [-15, -10, -5, 0, 5, 10, 15, 20, 25, 30, 35, 40, 45, 50, 55, 60]$. Hence, the Stanford score associated with a mutation is defined as follows:

$$S_m = \frac{\min\{s_{m,1}, \dots, s_{m,d}, \dots, s_{m,D}\}}{\|s\|}, \text{ with } d \in h$$

The weight to be given to mutation m is defined as follows.

$$w_m = \frac{Area_{VL}}{1 + e^{\alpha+\beta t} - \tanh(S_m)} \quad (1)$$

where t is the time passed (in days) between the last time the mutation m was detected and the start of the therapy of interest z . I.e., an increase in viral load increases the maximum weight of the mutation, and the Stanford score decreases the effect of fast and steep descent of the weight. Using this method to weigh mutations, a linear SVM model was trained to obtain a model of predictions of treatment success and keep the results interpretable.

Experiments and results

The EuResist integrated database

The Euresist Integrated Database EIDB is one of the world's largest databases regarding drug resistance in HIV-infected patients, both treatment-naïve and treated, undergoing clinical follow-up since 1998 [28]. The data comprises nine national cohorts from Italy, Germany, Sweden, Portugal, Spain, Luxembourg, Belgium, Turkey, and Russia. Recently, data from patients referred to facilities in Ukraine and Georgia have been added. The EuResist Database was established in 2006, to collect, in an anonymized form, data on demographic and clinical characteristics of PLWH, such as antiretroviral therapies, reasons for changing therapy, treatment responses, CD4+ cell counts, AIDS-defining events, and viral co-infections.

We trained a model to predict the success or failure of antiretroviral treatments for patients who could be either treatment-naïve or already treated. The predictors in the

model are the cumulative sequence of the predominant viral strains in patients' blood collected by all genotypic resistance tests (GRTs) performed before the start of the therapy of interest, information on mutations as downloaded from the Stanford HIVDB, viral load (VL) measurements as viral RNA copies per *ml* of blood plasma (*cp/ml*), and the individual drugs used in the therapies. The response is the therapy outcome. It should be emphasized that the clinical data available is not necessarily complete.

The dataset

The database contains data from 105, 101 PLWH but, for many of these patients, no consistent information is available to be used for our analysis. For example, nearly 8% of patients (8, 346) do not have data on VLs, GRTs, or therapies with a valid date.

The model is *therapy-oriented*, which means that we organize the data in terms of *patient-therapy pairs*. In the context of analyzing treatment success or failure, the notion of the tuples *patient-treatment episode* (PTE) and *patient-treatment change episode* (PTCE) has been defined [41].

Definition Patient-treatment episode. A patient-treatment episode (PTE) consists of a genotype (reverse transcriptase (RT), protease (PR) and/or integrase (IN)) at baseline, the set of pharmacologic compounds used in antiretroviral treatment, (cART), an optional VL at baseline, obtained no earlier than 90 days before treatment initiation, and follow-up VLs, referred to a patient. Patient-treatment episodes include both patients at first-line therapies and patient-treatment change episodes.

Definition Patient-treatment change episode. A patient treatment modification episode (PTCE) is a type of PTE. It refers to a period during which data are collected to assess how the patient responds to the change in ART that has become necessary for some reason such as virologic failure, toxicity, drug interactions, or simplification of therapy. The start of the new treatment regimen serves as the "baseline," and the period considered is divided into two blocks, before and after it. During this episode, it is necessary to closely monitor the patient's HIV viral load and genotype at baseline and in the follow-up period and any possible side effects.

Response to drug treatment is indicated with an outcome label $y \in \{0, 1\}$ indicating success or failure, respectively, according to a new EuResist Standard Datum definition that differs from the one used in the past.

Definition Standard Datum. Treatment success can be determined with a follow-up VL and optionally a VL at baseline as described. Follow-up VLs between 20 and 28 weeks after the start of therapy and the VL whose measurement date is closer to twenty-four weeks after the start of therapy are considered. Below, PTEs are referred to as successes, if the respective follow-up VL is less than 50 copies of HIV-1 RNA per milliliter of blood plasma. Otherwise, treatment is considered a failure. Cases in which treatment was changed before 24 weeks are considered as follows:

- Therapy lasting at most 4 weeks: excluded because most likely discontinued due to toxicity;
- Therapy lasting 4 to 8 weeks: success if it has viral load below 50 cps/ml or at least 1 log decrease in viral load in the most recent detection, otherwise failure;
- Therapy lasting 8 to 20 weeks: success if it has viral load below 50 cps/ml or at least 2 log decrease in viral load in the most recent detection, otherwise, failure.

The tests for viremia have become more sensitive in recent years. Lower thresholds than previously ([41, 40]) can now be used to determine therapy success. This is also more consistent with the current clinical practices.

In order to be included in the analysis, a patient-therapy pair must meet the following criteria:

1. The patient-therapy pair must comply with the definition of PTE, in particular, the full list of the compounds used in the therapy, at least one genotypic sequence before the start date of therapy and the follow-up VL must be present.
2. The patient that is administered that therapy must have at least one VL recorded before and after each GRT documented by a sequence at any temporal distance so that VL interpolation curves can be constructed.
3. The patient's therapy must be able to be judged successful or unsuccessful based on the definition of the standard datum.

For each data point (patient-therapy pair), viral genotype information is provided in terms of a binary vector indicating the presence (1) or absence (0) of mutations, multiplied by weights to account for the patient's history, as described in the *The weighting factors of the mutations* section. The therapy to be administered next is also coded by a binary vector indicating the presence or absence of the drugs appearing in the dataset. The full list of drugs considered are listed in the supplemental material.

We consider both polymorphic and non-polymorphic mutations in our model. Polymorphisms are mutations occurring in at least 1% of viruses not exposed to selective drug pressure, i.e., reflecting natural diversity independent from therapy. A nonpolymorphic mutation does not occur in the absence of therapy [29]. The choice of considering all the mutations stems from the fact that there may be mutations or combinations thereof that can result in reduced susceptibility of the virus to a cART or act on the fitness of the virus, not yet recognized as such. In the end, our training set includes 22,000 patient-therapy pairs, including 12,386 successes and 9,614 failures.

The trained models

Because of the way the PTEs and PTCEs are defined, it is possible for multiple records in the dataset with different therapies to pertain to the same patient with different therapies. The *Full* dataset has 22,000 *patient-therapy* pairs (12,386 successes and 9,614 failures), referring to 10,540 patients.

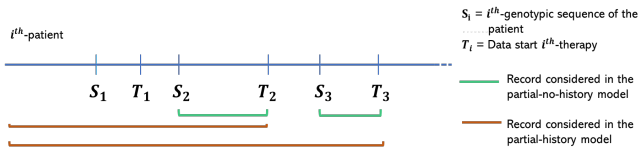


Figure 3: Therapies and relative patient history considered in the history model and in the no-history model

We want to understand whether the history of mutations with their viral loads, recorded when these mutations appeared, is relevant. Hence, two datasets that only include therapies with at least two previous GRTs, were created. In this way, the *patient-therapy* pairs considered refer patients with a history that one can decide to use or not in the model. This filtering resulted in two smaller datasets of 10,581 *patient-therapy* pairs (5,415 successes and 5,166 failures). The difference between the two *partial* dataset are the following:

- *Partial_History_weighted dataset*: for each *patient-therapy* pair, all GRTs previous to the predicted therapy are considered and mutation are weighted by the degression weight.
- *Partial_No-history_Non-weighted dataset*: for each *patient-therapy* pair, only the last GRT collected before the start of therapy is considered, and the mutations detected in the GRT are considered in binary form.

Figure 3 illustrates the therapies considered in the two datasets. Therapy T_1 is not considered because, prior to that therapy there is only one genotype at baseline. Without making this selection, in the model trained on the full dataset, therapies without history (only one previous GTR) would have deluded our analysis.

Next, four additional datasets were built using the *Full* set of 22,000 patient-therapy pairs. The aim is to consider in the final model both therapies with a history and first-line and follow-up therapies for which no previous history is available (missing data). These datasets will be called *Full_(history/no-history)_(weighted/non-weighted)* datasets. The qualifiers *history*, *No-history*, *weighted* and *Non-weighted* have the same meaning as in the previous datasets. While *history* considers not only the last GRT, but mutations from all the available GRTs previous to the therapy, *weighted* uses weighted instead of binary input.

Overall, we consider six datasets. The models trained on these datasets are named after them. Table 2 of supplementary material presents a schematic view of the datasets' characteristics.

Experimental setting

The *full* datasets are slightly unbalanced: 56.3% of the records pertain to successes. For the *partial* datasets, the respective fraction is 51.17%.

The data were randomly divided into training set (75%) and test set (25%). To avoid data leakage, therapies belonging

to the same patient were included in the same set. A linear Support Vector Machine for classification was trained to predict success, or failure labels based on outputs representing probability estimates [24]. A random search of the hyperparameters was carried out in order to set the parameters for the best possible performance. Values of hyperparameters were sampled from a probability distribution, and the performance of the resulting models was evaluated by a five times five-fold cross-validation. In this way, for each parameter setting, we obtain 25 performance values of the model with that setting when using different training and validation sets. In particular, the regularization parameter C was sampled from a log-uniform distribution ($C \sim U(e^{-14}, 1)$). For each cross-validation set, the model with the lowest value of C whose average performance (in terms of ROC-AUC score) was not significantly lower than the best average performance was selected (Benjamini-Hochberg-corrected Wilcoxon signed-rank test [38] with a significance threshold of 0.05). For the mutations for which no data was available to fit the parameter θ of the sigmoid curve, θ was treated as a hyperparameter of the model, sampled uniformly between the minimum and the maximum value of the parameters α and β learned for the mutations of the same drug class.

Results

Model performances were compared performing the Nadeau and Bengio statistical test [15] on ROC-AUC scores, with a significance level of 5%.

Partial_model results. The results obtained from the two models based on the partial datasets are shown in Table 1. The *Partial_history_weighted model* achieves almost two percentage points more in ROC-AUC score than the *Partial_No-history_Non-weighted model*, showing a statistically significant difference between the two approaches.

Full_model results. Table 2 shows the results obtained using the four models based on the full datasets. Thanks to the availability of more data points, the models obtain better results overall compared to the partial models. In particular, the *Full_history_weighted model* reaches the highest ROC-AUC score of 76.34% (± 0.099), indicating its superior ability to predict treatment outcomes accurately. The p-values associated with the ROC-AUC scores of the other models, when compared with the *Full_history_weighted model*, further reinforce the statistical significance of the difference in performance.

To further analyze the impact of historical information, additional statistical analysis was conducted to compare the impact of incorporating historical information. Specifically, an attempt was made to compare the performance of the *Full_history_weighted* (H) model and the *Full_No-history_Non-weighted* (NH) model. This comparison aimed to evaluate the influence of historical information on the predictive accuracy of the models. Table 3 presents the mean

Model	AUC
<i>Partial_history_weighted</i>	72.42% (± 0.140)
<i>Partial_No-history_Non-weighted</i>	70.43% (± 0.139) * _{0.0011}

indicates the p-value w.r.t. the history_weighted model

Table 1

Performance metrics of models trained with the partial dataset that only considers patients for which historical information is available.

Model	AUC
<i>Full_history_weighted</i>	76.34% (± 0.099)
<i>Full_No-history_weighted</i>	76.13% (± 0.099) * _{0.0064}
<i>Full_history_Non-weighted</i>	74.67% (± 0.100) * _{1.02e-32}
<i>Full_No-history_Non-weighted</i>	74.98% (± 0.098) * _{6.92e-23}

indicates the p-value w.r.t. the history_weighted model

Table 2

Performance metrics of models trained with the full dataset that considers both first-line therapy patients and treatment-experienced patients.

and standard deviation of predicted probabilities for treatment successes and failures, ranked according to whether or not historical information was considered. Notably, when only treatments with a history (indicated with a ✓) are considered, the H-model consistently outperforms the NH-model in predicting the probabilities of both success and failure. This suggests that incorporating historical information provides valuable insights for accurate prediction.

Wilcoxon tests were performed on the probability distributions of treatment outcomes between the H-model and NH-model to assess the statistical differences between the probabilities predicted by the two models. The test hypothesis is given in Table 4. Results show significant differences between the H and NH models. For both failures, with and without historical information, the H-model outperforms the NH-model, as evidenced by the remarkably low p-values ($5.32e^{-16}$ and $9.03e^{-25}$, respectively). Regarding all treatment successes, the H-model significantly outperforms the NH-model, with a p-value of $7.15e^{-6}$. However, when narrowing down the analysis to only successes with historical information, the high p-value (0.9536) indicates that the null hypothesis that the H-model predicts smaller or equal probabilities than the NH-model cannot be rejected.

Figure 4 displays the H and NH-model's predicted probability distributions, divided for successes and failures. The cut-off for probabilities are represented for both models. For each model, the part of the line above its cut-off represents therapies correctly classified by the model, while the portion below shows therapies incorrectly classified. In general, H-model seems to predict higher probabilities than the NH-model. Focusing on failures, Figure 4a shows that the H-model correctly classifies more failures than the NH-model. Looking at the space between the two cut-offs, where failures

Type of therapies correctly classified	Type of model	Only therapy with history	Mean \pm SD of predicted probabilities
Successes	H	✓	0.720 \pm 0.11
Successes	NH	✓	0.699 \pm 0.20
Failures	H	✓	0.699 \pm 0.12
Failures	NH	✓	0.677 \pm 0.099
Successes	H	×	0.724 \pm 0.106
Successes	NH	×	0.700 \pm 0.115
Failures	H	×	0.667 \pm 0.119
Failures	NH	×	0.665 \pm 0.098

indicates the p-value w.r.t. the history_weighted model

Table 3

Mean and standard deviation of predicted probabilities by the two models, divided by type of therapy (success or failure). The column "only therapy with history" is valued with ✓ when only therapies with more than one previous genotype are considered or with × when all the therapies are considered.

Wilcoxon test Between H and NH probability distribution for:	P-VALUE
successes $H_0 : p(\text{Success}_H) \leq p(\text{Success}_{NH})$	7.15e⁻⁶
successes with history $H_0 : p(\text{Success}_H) \leq p(\text{Success}_{NH})$	0.9536
failures $H_0 : p(\text{Failure}_H) \leq p(\text{Failure}_{NH})$	5.32e⁻¹⁶
failures with history $H_0 : p(\text{Failure}_H) \leq p(\text{Failure}_{NH})$	9.03e⁻²⁵

indicates the p-value w.r.t. the history_weighted model

Table 4

p-values of the Wilcoxon tests performed on the predicted probability distributions of the models, with the null hypothesis H_0 .

are correctly classified by the H-model but not by the NH-model, the H's probabilities are slightly higher. Segments below the lower cut-off represent misclassified failures by both models, with comparable probability distributions. Focusing on successes, Figure 4b shows fewer successes classified correctly by the H-model than the NH-model. However, the probabilities predicted by the H-model are higher, even for successes only correctly classified by the NH-model. NH-model's probabilities are higher for misclassified successes represented by lines below the lower cut-off.

Discussion

We have conducted several statistical analyses to compare the impact of incorporating historical information. Models employing *partial* datasets, including only patient-therapy pairs with relevant medical history before the target therapy, exhibit significant differences in the results. These

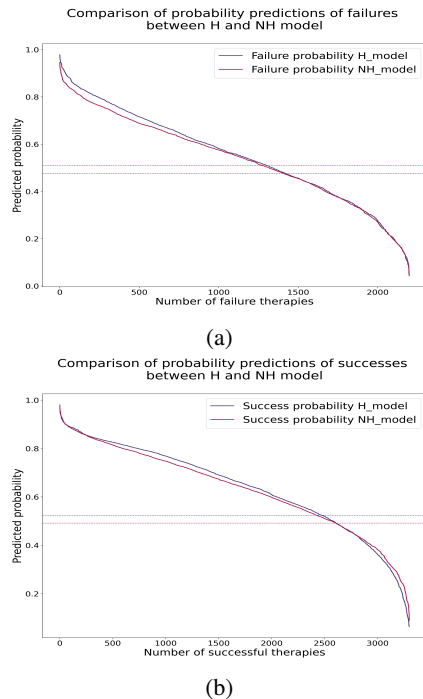


Figure 4: Plots of the probability distributions predicted by the models, respectively (a) for successes and (b) for failures. On the x-axis, there is the number of therapies, and on the y-axis, the models' predicted probabilities. The blue and red dotted lines represent the cut-offs for probabilities, respectively, for the H and NH-model. For each model, the portion of the line above its cut-off represents therapy correctly classified by the model, while the one below represents therapy incorrectly classified by the model.

underscore the importance of incorporating a patient's history into predictions of treatment outcomes, especially when eliminating the bias associated with therapies that lack the previous history.

Deeper analyses were conducted on the *full* models for the importance of training on *full* datasets. This includes both patient-therapy pairs with relevant medical history before the target therapy and patients without historical information. The latter could be patients with limited data or on first-line therapy. Ensuring accurate predictions for both categories is essential to provide valuable insights for clinical decision-making. The *Full_History_weighted model* (H) model has a higher ROC-AUC score (76.34%) than the *Full_No-history_No-weighted model* (NH) (74.98%). Interestingly, the *Full_No-history_weighted model* demonstrates performance comparable to the *Full_History_weighted model*. Both the models take historical information into account to some extent: the former because it considers the mutations of all the GRTs performed in the past by the patients weighted as explained earlier; the latter because, although only the last GRT is considered, the mutations are weighted taking into account the elapsed time since the mutation was detected, that is the date on which the genotype was sequenced. This suggests that the substantial improvements observed in the

history-weighted model are mainly attributed to incorporating the weighting factors rather than including historical mutations per se.

One reason why the H-model has better predictive performance than the NH-model, especially in the case of failures, could be attributed to the possibility that historical mutations represent latent reservoirs for HIV. Latent reservoirs are cells infected with the virus but in tissues other than blood serum. These remain inactive or dormant, evading the body's immune response to standard ART. The existence of latent reservoirs makes it difficult to eradicate HIV from the body because these cells can reactivate and generate new viral particles, leading to a reappearance of the virus and treatment failure. Presumably, the model, considering weighted historical mutations, can capture the intricate relationship between latent reservoirs and response to therapy, improving predictive performance in case of treatment failure.

Our study's implications align with a concept emerging from a recent study conducted by part of our team to study mutational history in a different context [21]. In this work, data from various patients are used cross-sectionally rather than longitudinally to infer the accumulation of mutations in multidrug-resistant patients, i.e., the order in which mutations occur over time (mutational history). Therefore, the respective model can predict aspects of mutational history from current genotypes. For example, if we observe a genotype with the X mutation and not with the Y mutation, but in the mutational history, Y was observed before X, Pirkl et al. 2023 hypothesize that the Y mutation may now be present only in the latent reservoir genotypes and not in the blood serum and that mutations are still present in the latent reservoir and thus have an impact on future therapies. Both studies emphasize the importance of mutations that occurred in the past for future therapies and drug resistance, respectively.

In conclusion, our study sheds light on the fact that incorporating the temporal dynamics of mutations improves prediction accuracy compared with the standard analysis of only the last available genotype. The results underscore the importance of considering the temporal aspect of mutations and their potential influence on treatment outcomes. They provide valuable insights into the complex dynamics of HIV infection, guiding future research and informing the development of effective therapeutic strategies.

Limitations of our work include the potential suboptimality of the constructed weighting factor for mutations, which combines VL magnitude, mutation timing, and duration, without a clear understanding of the individual influences of these three aspects. Furthermore, although the differences in performance between the models that include history and those that do not are statistically significant, the ROC-AUC of the non-history models is relatively high. This could be due to the methodology used to include history or the inherent incompleteness of the available data.

Competing interests

No competing interest is declared.

Author contributions statement

G.D.T, M.P, R.K., L.P, M.Z., T.L. conceptualized the study. G.D.T., F.L., I.V, and A.S. managed data curation and access. G.D.T. processed the data and conducted the statistical analysis under the supervision of all the authors. G.D.T., M.P., R.K., M.Z., and T.L. interpreted the results. G.D.T. wrote the manuscript. M.P., M.Z., L.P. and T.L. reviewed the manuscript. All authors have read and agreed to the published version of the manuscript.

Acknowledgments

The authors would like to thank the EuResist Network working group for their valuable work for the EIDB.

Data availability statement

Restrictions apply to the availability of these data. Data were obtained from the EuResist Network and are available for request through a study application form at <https://www.euresist.org/become-a-partner> with the permission of the EuResist Network.

Ethic statement

Ethical approval was granted in the host countries of the respective original databases contributing data to EIDB.

References

- [1] Altmann, A., Däumer, M., Beerenwinkel, N., Peres, Y., Schülter, E., Büch, J., Rhee, S.Y., Sönnernborg, A., Fessel, W.J., Shafer, R.W., Zazzi, M., Kaiser, R., Lengauer, T., 2009. Predicting the response to combination antiretroviral therapy: retrospective validation of geno2pheno-THEO on a large clinical database. *J. Infect. Dis.* 199, 999–1006.
- [2] Beerenwinkel, N., Däumer, M., Oette, M., Korn, K., Hoffmann, D., Kaiser, R., Lengauer, T., Selbig, J., Walter, H., 2003. Geno2pheno: Estimating phenotypic drug resistance from HIV-1 genotypes. *Nucleic Acids Res.* 31, 3850–3855.
- [3] Betancor, G., Nevot, M., Mendieta, J., Gómez-Puertas, P., Martínez, M.A., Menéndez-Arias, L., 2014. Molecular basis of the association of H208Y and thymidine analogue resistance mutations M41L, L210W and T215Y in the HIV-1 reverse transcriptase of treated patients. *Antiviral Res.* 106, 42–52.
- [4] Ciccullo, A., Borghi, V., Giacomelli, A., Cossu, M.V., Sterrantino, G., Latini, A., Giacometti, A., De Vito, A., Gennari, W., Madeddu, G., Capetti, A., d'Ettorre, G., Mussini, C., Rusconi, S., Di Giambenedetto, S., Baldin, G., 2021. Five years with dolutegravir plus lamivudine as a switch strategy: Much more than a positive finding. *J. Acquir. Immune Defic. Syndr.* 88, 234–237.
- [5] Cozzi-Lepri, A., Noguera-Julian, M., Di Giallonardo, F., Schurman, R., Däumer, M., Aitken, S., Ceccherini-Silberstein, F., D'Arminio Monforte, A., Geretti, A.M., Booth, C.L., Kaiser, R., Michalik, C., Jansen, K., Masquelier, B., Bellecave, P., Kouyos, R.D., Castro, E., Furrer, H., Schultze, A., Günthard, H.F., Brun-Vezinet, F., Paredes, R., Metzner, K.J., CHAIN Minority HIV-1 Variants Working Group, 2015. Low-frequency drug-resistant HIV-1 and risk of virological failure to first-line NNRTI-based ART: a multicohort european case-control study using centralized ultrasensitive 454 pyrosequencing. *J. Antimicrob. Chemother.* 70, 930–940.
- [6] Davidson, C.J., Zerlinger, E., Champion, K.J., Gauthier, M.P., Wang, F., Boonyaratanakornkit, J., Jones, J.R., Schreiber, E., 2012. Improving the limit of detection for sanger sequencing: a comparison of methodologies for KRAS variant detection. *Biotechniques* 53, 182–188.
- [7] Fox, E.J., Reid-Bayliss, K.S., Emond, M.J., Loeb, L.A., 2014. Accuracy of next generation sequencing platforms. *Next Gener. Seq. Appl.* 1.
- [8] Gagliardini, R., Ciccullo, A., Borghetti, A., Maggiolo, F., Bartolozzi, D., Borghi, V., Pecorari, M., Di Biagio, A., Callegaro, A.P., Bruzzone, B., Saladini, F., Paolucci, S., Maserati, R., Zazzi, M., Di Giambenedetto, S., De Luca, A., Mellace, V., Capetti, A., Rita Gismondo, M., Luisa Biondi, M., Mussini, C., Pecorari, M., Gianotti, N., Sacchini, D., Parruti, G., Polilli, E., Baldelli, F., Zanussi, S., Nerli, A., Lenzi, L., Calzetti, C., Vivarelli, A., Maserati, R., Baldanti, F., Poletti, F., Mondino, V., Malena, M., Cascio, A., Filice, G., Magnani, G., Zerbini, A., Lombardi, F., Di Giambenedetto, S., Andreoni, M., Montano, M., Vullo, V., Turriziani, O., Zazzi, M., Gonnelli, A., De Luca, A., Boeri, E., Bonora, S., Ghisetti, V., Francisci, D., Grossi, P., Bagnarelli, P., Butini, L., del Gobbo, R., Giacometti, A., Tacconi, D., Monno, L., Punzi, G., Callegaro, A., Maggiolo, F., Zoncada, A., Paolini, E., Sighinolfi, L., Colao, G., Corsi, P., Blanc, P., Galli, L., Meraviglia, P., Tosti, A., Bruzzone, B., Setti, M., Penco, G., Di Biagio, A., Nencioni, C., Pardelli, R., Arcidiacono, I., Degiuli, A., De Gennaro, M., Soria, A., Focà, A., Surace, L., Cosco, L., Malandrini, S., Milini, P., Cicconi, P., Rusconi, S., Micheli, V., ARCA Study Group, 2018. Impact of the M184V resistance mutation on virological efficacy and durability of lamivudine-based dual antiretroviral regimens as maintenance therapy in individuals with suppressed HIV-1 RNA: A cohort study. *Open Forum Infect. Dis.* 5.
- [9] Girouard, M., Diallo, K., Marchand, B., McCormick, S., Götte, M., 2003. Mutations E44D and V118I in the reverse transcriptase of HIV-1 play distinct mechanistic roles in dual resistance to AZT and 3TC. *J. Biol. Chem.* 278, 34403–34410.
- [10] Hachiya, A., Gatanaga, H., Kodama, E., Ikeuchi, M., Matsuo, M., Harada, S., Mitsuya, H., Kimura, S., Oka, S., 2004. Novel patterns of nevirapine resistance-associated mutations of human immunodeficiency virus type 1 in treatment-naïve patients. *Virology* 327, 215–224.
- [11] Langford, S.E., Ananworanich, J., Cooper, D.A., 2007. Predictors of disease progression in HIV infection: a review. *AIDS Res. Ther.* 4, 11.
- [12] Larder, B., Wang, D., Revell, A., Montaner, J., Harrigan, R., De Wolf, F., Lange, J., Wegner, S., Ruiz, L., Pérez-Elias, M.J., Emery, S., Gatell, J., Monforte, A.D., Torti, C., Zazzi, M., Lane, C., 2007. The development of artificial neural networks to predict virological response to combination HIV therapy. *Antivir. Ther.* 12, 15–24.
- [13] Lengauer, T., Sing, T., 2006. Bioinformatics-assisted anti-HIV therapy. *Nat. Rev. Microbiol.* 4, 790–797.
- [14] Liu, P., You, Y., Liao, L., Feng, Y., Shao, Y., Xing, H., Lan, G., Li, J., Ruan, Y., Li, D., 2022. Impact of low-level viremia with drug resistance on CD4 cell counts among people living with HIV on antiretroviral treatment in china. *BMC Infect. Dis.* 22, 426.
- [15] Nadeau, C., Bengio, Y., 1999. Inference for the generalization error, in: Solla, S., Leen, T., Müller, K. (Eds.), *Advances in Neural Information Processing Systems*, MIT Press. URL: <https://proceedings.neurips.cc/paper/1999/file/7d12b66d3df6af8d429c1a357d8b9e1a-Paper.pdf>.
- [16] Nebbia, G., Sabin, C.A., Dunn, D.T., Geretti, A.M., UK Collaborative Group on HIV Drug Resistance, UK Collaborative HIV Cohort (CHIC) Study Group, 2007. Emergence of the H208Y mutation in the reverse transcriptase (RT) of HIV-1 in association with nucleoside RT inhibitor therapy. *J. Antimicrob. Chemother.* 59, 1013–1016.
- [17] Obermeier, M., Pironti, A., Berg, T., Braun, P., Däumer, M., Eberle, J., Ehret, R., Kaiser, R., Kleinkauf, N., Korn, K., Kücherer, C.,

- Müller, H., Noah, C., Stürmer, M., Thielen, A., Wolf, E., Walter, H., 2012. HIV-GRADE: a publicly available, rules-based drug resistance interpretation algorithm integrating bioinformatic knowledge. *Intervirology* 55, 102–107.
- [18] Organization, W.H., 2023. World health statistics 2023: monitoring health for the SDGs, sustainable development goals. World Health Organization.
- [19] Pao, D., Andrady, U., Clarke, J., Dean, G., Drake, S., Fisher, M., Green, T., Kumar, S., Murphy, M., Tang, A., Taylor, S., White, D., Underhill, G., Pillay, D., Cane, P., 2004. Long-term persistence of primary genotypic resistance after HIV-1 seroconversion. *J. Acquir. Immune Defic. Syndr.* 37, 1570–1573.
- [20] Paredes, R., Tzou, P.L., van Zyl, G., Barrow, G., Camacho, R., Carmona, S., Grant, P.M., Gupta, R.K., Hamers, R.L., Harrigan, P.R., Jordan, M.R., Kantor, R., Katzenstein, D.A., Kuritzkes, D.R., Maldarelli, F., Otelea, D., Wallis, C.L., Schapiro, J.M., Shafer, R.W., 2017. Collaborative update of a rule-based expert system for HIV-1 genotypic resistance test interpretation. *PLoS One* 12, e0181357.
- [21] Pirkil, M., Büch, J., Devaux, C., Böhm, M., Sönnnerborg, A., Incardona, F., Abecasis, A., Vandamme, A.M., Zazzi, M., Kaiser, R., Lengauer, T., Group, T.E.N.S., 2023. Analysis of mutational history of multidrug-resistant genotypes with a mutagenetic tree model. *Journal of Medical Virology* 95, e28389. URL: <https://onlinelibrary.wiley.com/doi/abs/10.1002/jmv.28389>, doi:<https://doi.org/10.1002/jmv.28389>, arXiv:<https://onlinelibrary.wiley.com/doi/pdf/10.1002/jmv.28389>.
- [22] Pironti, A., Pfeifer, N., Walter, H., Jensen, B.E.O., Zazzi, M., Gomes, P., Kaiser, R., Lengauer, T., 2017a. Using drug exposure for predicting drug resistance – a data-driven genotypic interpretation tool. *PLOS ONE* 12, 1–27. URL: <https://doi.org/10.1371/journal.pone.0174992>, doi:[10.1371/journal.pone.0174992](https://doi.org/10.1371/journal.pone.0174992).
- [23] Pironti, A., Walter, H., Pfeifer, N., Knops, E., Lübke, N., Büch, J., Di Giambenedetto, S., Kaiser, R., Lengauer, T., EuResist Network Study Group, 2017b. Determination of phenotypic resistance cutoffs from routine clinical data. *J. Acquir. Immune Defic. Syndr.* 74, e129–e137.
- [24] Platt, J., 1999. Probabilistic outputs for support vector machines and comparisons to regularized likelihood methods. *Advances in Large Margin Classifiers* 10.
- [25] Rhee, S.Y., Boehm, M., Tarasova, O., Di Teodoro, G., Abecasis, A.B., Sönnnerborg, A., Bailey, A.J., Kireev, D., Zazzi, M., the EuResist Network Study Group, Shafer, R.W., 2022. Spectrum of atazanavir-selected protease inhibitor-resistance mutations. *Pathogens* 11. URL: <https://www.mdpi.com/2076-0817/11/5/546>, doi:[10.3390/pathogens11050546](https://doi.org/10.3390/pathogens11050546).
- [26] Riemenschneider, M., Hummel, T., Heider, D., 2016. Shiva - a web application for drug resistance and tropism testing in hiv. *BMC Bioinformatics* 17.
- [27] Romano, L., Venturi, G., Bloor, S., Harrigan, R., Larder, B.A., Major, J.C., Zazzi, M., 2002. Broad nucleoside-analogue resistance implications for human immunodeficiency virus type 1 reverse-transcriptase mutations at codons 44 and 118. *J. Infect. Dis.* 185, 898–904.
- [28] Rossetti, B., Incardona, F., Di Teodoro, G., Mommo, C., Saladini, F., Kaiser, R., Sönnnerborg, A., Lengauer, T., Zazzi, M., 2023. Cohort profile: A european multidisciplinary network for the fight against hiv drug resistance (euresist network). *Tropical Medicine and Infectious Disease* 8. URL: <https://www.mdpi.com/2414-6366/8/5/243>, doi:[10.3390/tropicalmed805243](https://doi.org/10.3390/tropicalmed805243).
- [29] Shafer, R.W., Rhee, S.Y., Pillay, D., Miller, V., Sandstrom, P., Schapiro, J.M., Kuritzkes, D.R., Bennett, D., 2007. HIV-1 protease and reverse transcriptase mutations for drug resistance surveillance. *AIDS* 21, 215–223.
- [30] Suñé, C., Brennan, L., Stover, D.R., Klimkait, T., 2004. Effect of polymorphisms on the replicative capacity of protease inhibitor-resistant HIV-1 variants under drug pressure. *Clin. Microbiol. Infect.* 10, 119–126.
- [31] Tang, M.W., Liu, T.F., Shafer, R.W., 2012. The HIVdb system for HIV-1 genotypic resistance interpretation. *Intervirology* 55, 98–101.
- [32] Tang, M.W., Shafer, R.W., 2012. HIV-1 antiretroviral resistance: scientific principles and clinical applications. *Drugs* 72, e1–25.
- [33] Tsiatis, A.C., Norris-Kirby, A., Rich, R.G., Hafez, M.J., Gocke, C.D., Eshleman, J.R., Murphy, K.M., 2010. Comparison of sanger sequencing, pyrosequencing, and melting curve analysis for the detection of KRAS mutations: diagnostic and clinical implications. *J. Mol. Diagn.* 12, 425–432.
- [34] Vermeiren, H., Van Craenenbroeck, E., Alen, P., Bacheler, L., Picchio, G., Lecocq, P., Virco Clinical Response Collaborative Team, 2007. Prediction of HIV-1 drug susceptibility phenotype from the viral genotype using linear regression modeling. *J. Virol. Methods* 145, 47–55.
- [35] Vrancken, B., Trovão, N.S., Baele, G., van Wijngaerden, E., Vandamme, A.M., van Laethem, K., Lemey, P., 2016. Quantifying next generation sequencing sample pre-processing bias in HIV-1 complete genome sequencing. *Viruses* 8, 12.
- [36] Wensing, A.M., Calvez, V., Ceccherini-Silberstein, F., Charpentier, C., Günthard, H.F., Paredes, R., Shafer, R.W., Richman, D.D., 2022a. 2022 update of the drug resistance mutations in HIV-1. *Top. Antivir. Med.* 30, 559–574.
- [37] Wensing, A.M., Calvez, V., Ceccherini-Silberstein, F., Charpentier, C., Günthard, H.F., Paredes, R., Shafer, R.W., Richman, D.D., 2022b. 2022 update of the drug resistance mutations in HIV-1. *Top. Antivir. Med.* 30, 559–574.
- [38] Wilcoxon, F., 1945. Individual comparisons by ranking methods. *Biometrics* 1, 196–202.
- [39] Winters, B., Montaner, J., Harrigan, P.R., Gazzard, B., Pozniak, A., Miller, M.D., Emery, S., van Leth, F., Robinson, P., Baxter, J.D., Perez-Elias, M., Castor, D., Hammer, S., Rinehart, A., Vermeiren, H., Van Craenenbroeck, E., Bacheler, L., 2008. Determination of clinically relevant cutoffs for HIV-1 phenotypic resistance estimates through a combined analysis of clinical trial and cohort data. *J. Acquir. Immune Defic. Syndr.* 48, 26–34.
- [40] Zazzi, M., Incardona, F., Rosen-Zvi, M., Prosperi, M., Lengauer, T., Altmann, A., Sönnnerborg, A., Lavee, T., Schülter, E., Kaiser, R., 2012. Predicting response to antiretroviral treatment by machine learning: the EuResist project. *Intervirology* 55, 123–127.
- [41] Zazzi, M., Kaiser, R., Sönnnerborg, A., Struck, D., Altmann, A., Prosperi, M., Rosen-Zvi, M., Petroczi, A., Peres, Y., Schülter, E., Boucher, C.A., Brun-Vezinet, F., Harrigan, P.R., Morris, L., Obermeier, M., Perno, C.F., Phanuphak, P., Pillay, D., Shafer, R.W., Vandamme, A.M., van Laethem, K., Wensing, A.M.J., Lengauer, T., Incardona, F., 2011. Prediction of response to antiretroviral therapy by human experts and by the EuResist data-driven expert system (the EVE study). *HIV Med.* 12, 211–218.

Supplemental material

Details on the datasets

The drugs considered in the datasets are the following: lamivudine (3TC), abacavir (ABC), amprenavir (APV), atazanavir (ATV), zidovudine (AZT), bictegravir (BIC), cabotegravir (CAB), stavudine (D4T), zalcitabine (DDC), didanosine (DDI), delavirdine (DLV), doravirine (DOR), darunavir (DRV), dolutegravir (DTG), efavirenz (EFV), etravirine (ETR), elvitegravir (EVG), fosamprenavir (FPV), emtricitabine (FTC), indinavir (IDV), lopinavir (LPV), nelfinavir (NFV), nevirapine (NVP), raltegravir (RAL), rilpivirine (RPV), saquinavir (SQV), tenofovir alafenamide (TAF), tenofovir disoproxil (TDF), tipranavir (TPV).

Due to the definitions of PTEs (Patient-Treatment Episodes) and PTCEs (Patient-Treatment Change Episodes), it is feasible for various entries in the datasets, involving distinct treatments, to relate to a single patient undergoing different

# Therapies per patient	Label	# Patients
1	0	4659
1	1	3363
2	0	1781
2	1	1230
3	0	691
3	1	501
4	0	253
4	1	235
5	0	96
5	1	118
6	0	44
6	1	49
7	0	19
7	1	26
8	0	14
8	1	14
9	0	4
9	1	10
10	0	5
11	1	3
11	1	1
12	1	2
15	1	1

Table 5
Number of therapies per patient

therapies in different time periods. Table 5 reports how many therapies there are for the same patient, divided between successful (label 0) and failed therapies (label 1), according to the Standard Datum definition provided in the main text, in "The Dataset" Section. To guard against data leakage, either all therapies referring to the same patient were included in the training set or all of them were included in the test set.

Six different datasets have been built. A tabular form of listing the various models and datasets used in a simple visualization is presented in Table 6.

Significance test

To assess whether the history model performs better than the no-history model in terms of generalization capability, we use significance tests. The most common method for comparing the performance of Machine Learning models is the paired Student's t-test combined with random sub-sampling of the training set. However, one of the key assumptions of this test is that the underlying data be sampled independently from the two populations being compared. Since the models are trained on the same training set, the paired Student's t-test could lead to misleading results, with a high false positive rate (i.e., having a high probability of rejecting the null hypothesis indicating that the two models are significantly different, when this is in fact the case, i.e. overrating the significance of using history data). Nadeau and Bengio [15] propose a variance correction that accounts

for the dependence between the two. We apply their significance test in our analysis, with a significance level of 5%

Cut-off for the predicted probabilities

The trained models generate probabilities that indicate the likelihood of belonging to a certain class. Typically, a default threshold of 0.5 is used to assign class labels based on these probabilities. However, relying solely on this default threshold can lead to suboptimal performance, particularly when dealing with datasets that have unbalanced class distributions. Although, in our case, the overall dataset is not highly unbalanced, it is still helpful to adjust the threshold according to the characteristics of the training data.

A simple strategy was used to determine the most suitable threshold for mapping probabilities onto class labels. A comprehensive search was conducted with 1,000 threshold values equally spaced between 0 and 1. Through this iterative process, each model identified an individual threshold that maximized balanced accuracy. This ensures that the threshold is tailored to the specific characteristics of each model, finding a desirable compromise between sensitivity and specificity.

Through this iterative threshold selection approach, we improve model performance and obtain more accurate classification results. It allows us to effectively handle variations within the dataset and address situations where imbalances between classes may affect the model's predictive capabilities.

Analysis of the importance of mutations

Mutations ranking

Identifying the role of mutations in predicting the outcome of therapy is paramount for various reasons. The response of HIV to specific antiretroviral drugs can vary depending on the mutations present in its genome. Gaining an understanding of the role of mutations is crucial for improving treatment recommendations and maximizing treatment effectiveness. It allows us to identify mutations associated with drug resistance and comprehend how these mutations interact and impact viral suppression. This knowledge aids in selecting appropriate drug regimens that optimize treatment outcomes.

The model trained is a linear Support Vector Machine. The linear SVM provides hyperplane coefficients that represent the weights assigned to the features of the input data. These coefficients serve for assessing the importance and contributions of each feature in the SVM's decision-making process. The higher the absolute value of a mutation's coefficient, the more that mutation plays a role in determining the outcome. Moreover, we calculated individual weights for each mutation of each patient, as described in the main paper in the "Methods" section. When mutations are weighted low, at least one of the following conditions occurs: (i) they were observed far back in time, (ii) the patient's viral load, at the time of observing the mutation, was at low levels or undetectable, (iii) the Stanford score associated with the mutation is low. The low weight associated with a mutation

Model name	Possible # of GRTs > 1 prior to the target therapy	# of GRTs = 1 prior to the target therapy	Mutations of the GRT at baseline	The mutations of GRTs before the one at baseline	Binary vector of mutations	Weighted vector of mutations
<i>Partial_history_weighted</i>	✓	×	✓	✓	✓	✓
<i>Partial_No-history_Non-weighted</i>	✓	×	✓	×	✓	×
<i>Full_history_weighted</i>	✓	✓	✓	✓	✓	✓
<i>Full_No-history_weighted</i>	✓	✓	✓	×	✓	✓
<i>Full_history_Non-weighted</i>	✓	✓	✓	✓	✓	×
<i>Full_No-history_Non-weighted</i>	✓	✓	✓	×	✓	×

Table 6
Datasets and models' characteristics

suggests that the mutation does not play an essential role in determining therapy outcomes.

In studying the role of mutations, our objectives were twofold:

- To identify the mutations that consistently play a significant role in the model. These mutations consistently influence the outcome regardless of the specific context.
- To identify specific mutations that exhibit a high model coefficient despite having low weights in the model. Contrary to initial expectations, these mutations defy conventional evidence and demonstrate an important role in influencing the outcome.

For the first objective, we simply used the ranking of mutations obtained via the absolute values of the hyperplane coefficients. Inspecting Table 7 we can make interesting observations. For example, the top-ranking mutation is T200K. This mutation is not widely recognized as an important mutation for drug resistance in HIV but a few studies reported that T200K, even if it had not been reported previously, might be associated with NVP resistance [10]. In general, many of the top mutations in Table 7 are not recognized resistance mutations. Their coefficient values might be high because they were frequently observed near the start of the therapy of interest (i.e., the most recent genotype) and/or in the presence of a high viral load. Although most of the literature focuses on mutations that reduce viral fitness as something potentially exploitable in the clinic, these mutations could instead increase viral fitness and, thus, viral load.

For the second objective, a ranking formula was created to consider the potential discrepancy between the SVM hyperplane coefficient and the customized weights, allowing mutations with high coefficients but low weights to still receive a significant ranking value. The ranking formula for

each mutation m is the following:

$$\text{Ranking_value}_m = |\text{coefficient}_m|_{z_scaled} \cdot \left(- \sum_{i=1}^n \log w_m^i \right)_{z_scaled} \quad (2)$$

where *coefficient* is the SVM hyperplane coefficient, n is the size of the training set and w_m^i is the weight learned for mutation m of therapy-patient tuple i .

From this ranking, we identify 149 mutations that could play the role we aim for, which are the ones on the left of the dotted red line, representing the flexion point of the curve, in Figure 5b. The top-ranking 30 listed in Table 8. Some clinical considerations can be derived from this ranking. For example, L63P, among the first positions of the ranking, is usually not considered a significant mutation for drug resistance. However, it has been pointed out that (i) It is persistent and may remain even more than 18 months despite therapy changes [19], (ii) the mutation by itself does not render the virus resistant to inhibitors, but it does help the virus replicate more effectively, especially when under pressure from drugs. This suggests that small changes in the virus can have significant compensating effects, which could contribute to the evolution of drug-resistant variants of HIV-1 [30]. Indeed, most of the non-resistance mutations included in Table 8 have been implicated in compensatory or resistance modulation mechanisms. In PR, L10I, L63P, I93L even had a Stanford HIVdb score (although low) in past versions. The same applies to RTE44D and RTH208Y which have been studied in detail [27, 9, 3, 16]. Being aware that non-major mutations could increase viral fitness and have a compensatory effect that helps the virus replicate more effectively while not making the virus resistant to inhibitors per se, could have important implications for clinical practice. In particular, rule-based genotypic interpretation systems that consider only major resistance mutations may not be sufficient to design a therapy that considers all factors that play a role in the long-term efficacy of therapy.

Mutation	Value coefficient H model
RTT200K	0.3207
RTD113N	0.2964
INK14R	0.2819
RTT200V	0.2536
RTS322A	-0.2513
INM154I	-0.2466
RTK249R	-0.2434
RTK122Q	-0.2390
PRL63C	0.2278
RTM16V	-0.2258
RTE79K	-0.2235
PRV82S	0.2165
RTV245I	-0.2145
RTQ145E	0.2136
RTQ207H	-0.2095
PRG17D	0.2090
PRH69Y	0.2068
RTP176S	-0.2058
PRI93L	-0.1999
RTF227L	0.1977
RTS48P	0.1960
RTT215Y	0.1959
RTY271F	0.1950
RTE194D	-0.1939
RTV35E	0.1919
PRL90M	0.1914
RTL210S	0.1885
RTE248N	-0.1882
PRL19T	0.1878
INV37I	0.1862

Table 7

First 30 mutations of the ranking obtained ordering the mutations with descending absolute value of H model coefficients. The mutations name is preceded by PR (protease), RT (reverse transcriptase) or IN (integrase), depending on the region of the HIV genome. In bold, Stanford mutations.

Mutation	Ranking value
RTM184V	95.30
RTK103N	72.80
PRL90M	54.19
RTT215Y	49.21
RTK65R	33.17
RTD123E	30.88
RTK70R	30.86
PRL63P	28.02
PRI93L	26.13
RTK122E	21.81
RTM184I	20.33
RTK219Q	17.46
PRI84V	15.21
RTD67N	12.26
RTK277R	11.74
RTG196E	11.23
RTE44D	10.82
RTK49R	10.58
RTT215F	9.50
RTL210W	9.28
PRL10I	9.00
RTP294T	8.99
PRV82A	8.94
RTL100I	8.74
RTI202V	8.43
RTS162C	8.32
RTI293V	8.24
RTT286A	8.20
RTH208Y	7.88
PRI64V	7.81

Table 8

First 30 mutations of the ranking obtained ordering the mutations with descending ranking value computed as in 2. The mutations name is preceded by PR (protease), RT (reverse transcriptase) or IN (integrase), depending on the region of the HIV genome. In bold, Stanford mutations.

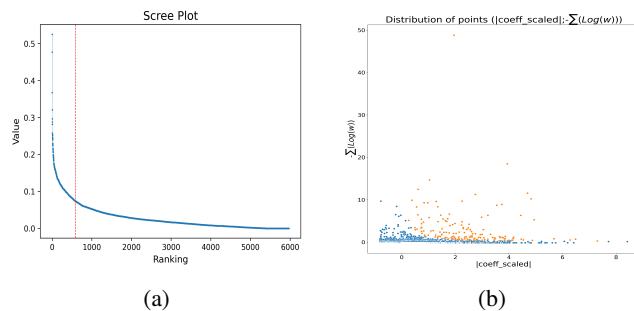


Figure 5: Figure (a) is the scree plot of the mutation, based on the ranking values obtained by 2. Figure (b) is the scatter plot of the points $(|coefficient_m|_{z_scaled}; -\sum_{i=1}^n \log w_m^i)$ to show that the ranking does not depend only to one of the two factors of the ranking formula but by both of them. The orange points are the mutations identified in the scree plot before the dashed red line that is the flexion point of the curve.

Enrichment analysis

An enrichment analysis of the mutations was performed. Enriched mutations are those that have become more widespread or common within a particular population or sample compared to their initial occurrence. The implication of mutations enriched could be (i) drug resistance: some mutations can provide pathogens with an advantage, enabling them to resist the effects of drugs or evade the immune system more effectively; (ii) disease progression: when a mutation becomes enriched, it may indicate an increased likelihood of developing drug resistance, potentially impacting the effectiveness of treatment and disease management. Enriched mutations could also be associated with increased virulence independently from drug resistance. The evolution of viral tropism over time is an example of this kind; (iii) functional implications: an enriched mutation suggests that the altered protein or gene variant provides some functional advantage or adaptation. This may enable individuals carrying the mutation to thrive or survive better in specific environments

or conditions.

To perform this analysis, Stanford tables on <https://hivdb.stanford.edu/cgi-bin/MutPrevBySubtypeRx.cgi> were used to look at whether the frequencies increase from Naïve patients to treatment-experienced patients (for HIV-subtype B, which is the subtype with the largest number of sequences available). We observe that 62% of the 147 selected mutations become enriched. This confirms that the approach we used in this work in treatment-experienced patients captured mostly biologically meaningful mutations, either conferring or modulating resistance. Importantly, one-third of the scored mutations do not appear to be enriched following treatment but may play a role for the clinical outcome. Mutations or polymorphisms of this kind may be associated with functional constraints limiting their selection under commonly used therapies yet play a role in response to treatment because of effects that are independent of drug resistance, e.g., impact on innate or adaptive immunity and fitness effects.